

# Endoplasmic reticulum (ER) luminal indicators in *Drosophila* reveal effects of HSP-related mutations on ER calcium dynamics

Megan K. Oliva<sup>1\*</sup>, Juan José Pérez-Moreno<sup>1</sup>, Jillian O'Shaughnessy<sup>1</sup>, Trevor J. Wardill<sup>2</sup>, Cahir J. O'Kane<sup>1\*</sup>

<sup>1</sup>University of Cambridge, United Kingdom, <sup>2</sup>Medical School, University of Minnesota, United States

*Submitted to Journal:*  
Frontiers in Neuroscience

*Specialty Section:*  
Neurodegeneration

*Article type:*  
Original Research Article

*Manuscript ID:*  
536116

*Received on:*  
18 Feb 2020

*Revised on:*  
24 Jun 2020

*Frontiers website link:*  
[www.frontiersin.org](http://www.frontiersin.org)

In review

---

### *Conflict of interest statement*

The authors declare that the research was conducted in the absence of any commercial or financial relationships that could be construed as a potential conflict of interest

### *Author contribution statement*

MKO performed all the cloning and Ca<sup>2+</sup> imaging experiments, and together with CJO'K designed the experiments. JJPM performed the confocal imaging acquisition. JO'S performed preliminary experiments and contributed to data analysis. TW provided initial training and support for Ca<sup>2+</sup> imaging experiments, and assisted in experimental design. The paper was written by MKO and CJO'K with comments and edits by JJPM, TJW and JO'S.

### *Keywords*

hereditary spastic paraplegia, Drosophila, Endoplasmic reticulum, calcium imaging, Neurodegeneration

### *Abstract*

Word count: 203

Genes for ER-shaping proteins are among the most commonly mutated in Hereditary Spastic Paraplegia (HSP). Mutation of these genes in model organisms can lead to disruption of the ER network. To investigate how the physiological roles of the ER might be affected by such disruption, we developed tools to interrogate its Ca<sup>2+</sup> signaling function. We generated GAL4-driven Ca<sup>2+</sup> sensors targeted to the ER lumen, to record ER Ca<sup>2+</sup> fluxes in identified Drosophila neurons. Using GAL4 lines specific for Type Ib or Type Is larval motor neurons, we compared the responses of different luminal indicators to electrical stimulation, in axons and presynaptic terminals. The most effective sensor, ER-GCaMP6-210, had a Ca<sup>2+</sup> affinity close to the expected ER luminal concentration. Repetitive nerve stimulation generally showed a transient increase of luminal Ca<sup>2+</sup> in both the axon and presynaptic terminals. Mutants lacking neuronal reticulon and REEP proteins, homologs of human HSP proteins, showed a larger ER luminal evoked response compared to wild type; we propose mechanisms by which this phenotype could lead to neuronal dysfunction or degeneration. Our lines are useful additions to a Drosophila Ca<sup>2+</sup> imaging toolkit, to explore the physiological roles of ER, and its pathophysiological roles in HSP and in axon degeneration more broadly.

### *Contribution to the field*

Hereditary Spastic Paraplegia (HSP) is a group of inherited neurodegenerative diseases characterized by progressive spasticity and weakness in the lower limbs. Whilst there have been many mutations identified in many genes in HSP, some of the most commonly mutated genes encode proteins that are involved in the shaping of the endoplasmic reticulum (ER) in neurons. Whilst recent research has revealed how lack of these genes can result in structural changes to ER in neurons, less is known about how these structural changes result in functional change to the neuron, and how this ultimately leads to degeneration. Therefore, to monitor one of the most important signalling components associated with ER, Ca<sup>2+</sup>, we generated flies that express ER-targeted sensors, to measure calcium fluxes in Drosophila. To demonstrate the utility of these fly lines we show that in a recently characterised Drosophila mutant for three HSP-related genes, ER calcium is increased in the mutant compared to WT at the presynaptic neuromuscular junction, in response to stimulation of the nerve. These lines will be useful for future studies in Drosophila to explore the physiological roles of ER, and its pathophysiological roles in HSP and in axon degeneration more broadly.

### *Funding statement*

This work was supported by grants BB/L021706 from the UK Biotechnology and Biological Sciences Research Council and MR/S011226 from the UK Medical Research Council to CJO'K. MKO was supported by a Newton International Fellowship (NF150362) from The Royal Society and a Marie Skłodowska-Curie Fellowship (701397) from the European Commission, JJPM was supported by a Marie Skłodowska-Curie fellowship (745007) from the European Commission.

*Ethics statements*

*Studies involving animal subjects*

Generated Statement: No animal studies are presented in this manuscript.

*Studies involving human subjects*

Generated Statement: No human studies are presented in this manuscript.

*Inclusion of identifiable human data*

Generated Statement: No potentially identifiable human images or data is presented in this study.

In review

*Data availability statement*

Generated Statement: This manuscript contains previously unpublished data. The name of the repository and accession number(s) are not available.

In review

## Endoplasmic reticulum (ER) luminal indicators in *Drosophila* reveal effects of HSP-related mutations on ER calcium dynamics

Authors: Megan K Oliva<sup>1\*</sup>, Juan José Perez-Moreno<sup>1</sup>, Jillian O'Shaughnessy<sup>1</sup>, Trevor J Wardill<sup>2</sup> and Cahir J O'Kane<sup>1\*</sup>

<sup>1</sup> Department of Genetics, University of Cambridge, Cambridge, UK

<sup>2</sup> College of Biological Sciences, University of Minnesota, Minneapolis, MN, USA

\*Correspondence:

Cahir J O'Kane, [c.okane@gen.cam.ac.uk](mailto:c.okane@gen.cam.ac.uk); and Megan K Oliva, [megan.oliva@gen.cam.ac.uk](mailto:megan.oliva@gen.cam.ac.uk)

Keywords: hereditary spastic paraplegia, endoplasmic reticulum, calcium imaging, *Drosophila*, neurodegeneration

### Abstract

Genes for ER-shaping proteins are among the most commonly mutated in Hereditary Spastic Paraplegia (HSP). Mutation of these genes in model organisms can lead to disruption of the ER network. To investigate how the physiological roles of the ER might be affected by such disruption, we developed tools to interrogate its Ca<sup>2+</sup> signaling function. We generated GAL4-driven Ca<sup>2+</sup> sensors targeted to the ER lumen, to record ER Ca<sup>2+</sup> fluxes in identified *Drosophila* neurons. Using GAL4 lines specific for Type Ib or Type Is larval motor neurons, we compared the responses of different luminal indicators to electrical stimulation, in axons and presynaptic terminals. The most effective sensor, ER-GCaMP6-210, had a Ca<sup>2+</sup> affinity close to the expected ER luminal concentration. Repetitive nerve stimulation generally showed a transient increase of luminal Ca<sup>2+</sup> in both the axon and presynaptic terminals. Mutants lacking neuronal reticulon and REEP proteins, homologs of human HSP proteins, showed a larger ER luminal evoked response compared to wild type; we propose mechanisms by which this phenotype could lead to neuronal dysfunction or degeneration. Our lines are useful additions to a *Drosophila* Ca<sup>2+</sup> imaging toolkit, to explore the physiological roles of ER, and its pathophysiological roles in HSP and in axon degeneration more broadly.

## Introduction

Hereditary Spastic Paraplegia (HSP) is a genetically heterogeneous disorder, with over 80 loci and 60 genes identified. It also shows phenotypic heterogeneity in manifestations such as age of onset, and the presence of other symptoms (Blackstone 2018). Despite this heterogeneity, there is evidence for some common mechanisms of cellular pathophysiology. The endoplasmic reticulum (ER) is implicated in these mechanisms, with HSP mutations affecting ER proteins with a variety of roles including lipid metabolism, ER membrane-contact-site function, and ER architecture (Blackstone 2018). Gene products that shape the tubular ER network are among the most commonly mutated in HSP, and mutation of these genes in model organisms leads to physical disruption of the ER network (O'Sullivan et al. 2012, Fowler and O'Sullivan 2016, Summerville et al. 2016, Yalçın et al. 2017, Lindhout et al. 2019). These studies point to the importance of a continuous and connected tubular ER network throughout axons and presynaptic terminals, and suggest disruption to this network as a common thread in HSP pathogenesis. Although changes in synaptic structure and function are found in these mutants (Summerville et al. 2016, Li et al. 2017, Lindhout et al. 2019), the direct physiological consequences of altered ER architecture remain elusive. It is imperative to understand the roles of ER architecture and the consequences of disrupting it, to understand how this might result in a neurodegenerative cascade.

We therefore need tools to study the physiological functions of axonal and presynaptic ER that depend on its architecture. Recently, de Juan-Sanz et al (2017) developed sensitive Genetically Encoded Calcium Indicators (GECIs) targeted to the ER lumen, to examine the role of the ER in  $Ca^{2+}$  handling and signaling in synaptic activity in mammalian cultured neurons. In parallel to our work, Handler et al. (2019) used one of these sensors (ER-GCaMP6-210) to detect  $Ca^{2+}$  release from the ER in mushroom body Kenyon cells. Here we have expressed this probe and two others with higher  $Ca^{2+}$  affinities under GAL4 control in *Drosophila* motor neurons. We show ER-GCaMP6-210 as the most effective reporter of the three by consistently producing the largest changes in fluorescent intensity, and characterize its localization and its reporting of stimulation-frequency-dependent ER  $Ca^{2+}$  fluxes in axon and presynaptic terminals. We then use it to show perturbation of  $Ca^{2+}$  handling in *Drosophila* in which ER organization is disrupted by loss of HSP-related ER-modeling proteins.

## Materials and Methods

### Gene Constructs

The *pUASTattB* vector (Bischof et al. 2007), was previously modified to include *attR* sites and the *ccdB* gene to make it compatible with the Gateway cloning system (Invitrogen) (Moreau et al. 2014). We further modified this vector, increasing the number of GAL4-binding sites from 5 to 17, to generate *p17xUASTattB*, and increase GAL4-dependent gene expression (Supplementary File 1). To generate *p17xUASTattB-ER-GCaMP6-210*, we PCR-amplified a fragment encoding GCaMP210-KDEL fused to a calreticulin signal peptide, from Addgene plasmid *ER-GCaMP6-210* (de Juan-Sanz et al. 2017) (Table 1), while adding *attB1* and *attB2* sites to its 5' and 3' ends to enable it to integrate into *p17xUASTattB* using the Gateway cloning system (Supplementary File 1). To generate *p17xUASTattB-CEPIA3-ER* and *p17xUASTattB-CEPIA4-ER*, we PCR-amplified the CEPIA coding region from Addgene plasmids *pCMV CEPIA3mt* and *pCMV CEPIA4mt* (Suzuki et al. 2014) (Table 1), while adding *attB1* and a BiP signal sequence to the 5' end, and HDEL and *attB2* to the 3' end (BiP and HDEL ER-targeting as in (Summerville et al. 2016)), and then integrating it into *p17xUASTattB* (Supplementary File 1).

### *Drosophila* Genetics

*p17xUASTattB-ER-GCaMP6-210*, *p17xUASTattB-CEPIA3-ER* and *p17xUASTattB-CEPIA4-ER* were injected into *Drosophila* embryos and integrated at landing site *attP86Fb* (Bischof et al. 2007) using phiC31 integrase-mediated integration, by the University of Cambridge Genetics Department injection service. Other fly stocks used can be found in Table 1.

### Histology

Third instar larvae were dissected in ice-cold  $\text{Ca}^{2+}$ -free HL3 solution (Stewart et al. 1994). HL3 was then replaced with PBS and larvae fixed for 10 min in PBS with 4% formaldehyde. Fixed preparations were mounted in Vectashield (Vector Laboratories), and images were collected using EZ-C1 acquisition software (Nikon) on a Nikon Eclipse C1si confocal microscope (Nikon Instruments, UK). Images were captured using a 40x/1.3NA oil objective.

### Live Imaging

Third instar larvae were dissected in ice-cold Schneider's insect medium (Sigma). Before imaging, Schneider's medium was replaced with HL3 containing (in mM) 70 NaCl, 5 KCl, 0.5  $\text{MgCl}_2$ , 10  $\text{NaHCO}_3$ , 115 sucrose, 5 trehalose, 5 HEPES, 1  $\text{CaCl}_2$  and 7 L-glutamic acid, pH  $\sim 7.2 \pm 0.05$ . The ER luminal response to electrical stimulation was sensitive to  $\text{Mg}^{2+}$ , with only

very small or no responses elicited in HL3 containing 20 mM MgCl<sub>2</sub>, which was used for fixed samples; a low-Mg<sup>2+</sup> HL3 solution (0.5 mM MgCl<sub>2</sub>) gave much more reliable responses.

Segmental nerves were cut with dissection scissors and then drawn by suction into a heat-polished glass pipette, ~10 µm internal diameter (Macleod et al. 2002), which was connected to a stimulator and train generator (DS2A-MK.II Constant Voltage Stimulator and DG2A Train/Delay Generator (Digitimer, Welwyn Garden City, UK)) to deliver supra-threshold electrical pulses (~5 V). Larval NMJ responses were recorded in abdominal segments A4-A6. After 10 s of baseline image acquisition, 400-µs impulses were delivered for 2 s at a range of frequencies. The interval between different stimulation frequencies was ~60 seconds, or until ER lumen fluorescence returned to baseline levels (whichever was longer).

Wide-field Ca<sup>2+</sup> imaging was performed on an upright Zeiss Axioskop2 microscope with Optosplit II (Cairn) using a 40x NA 1.0 water-immersion objective (W Plan-Apochromat 40x/1.0 DIC M27), a 2x C-Mount Fixed Focal Length Lens Extender (Cairn, Faversham, UK) and an Andor EMCCD camera (Model iXon Ultra 897\_BV, 512x512 pixels, Andor Technology, Belfast, UK) at 10 frames per second, 100 ms exposure, and EM gain level 100. Imaging data were acquired using Micro-Manager (Edelstein et al. 2014) and saved as multi-layer tif files before analysis using ImageJ FIJI (<https://fiji.sc>) (Schindelin et al. 2012).

### **Image analysis and Figure Preparation**

Confocal microscopy images of fixed samples were collected using EZ-C1 acquisition software on a Nikon Eclipse C1si confocal microscope. Images were analyzed and processed using ImageJ Fiji (<https://fiji.sc>) (Schindelin et al. 2012). Wide-field live images were opened in ImageJ Fiji, and channels were individually bleach-corrected (simple ratio, background intensity=0). Fluorescent intensity time courses were obtained for an ROI (region of interest) traced around the entire NMJ, or axon segment, in each frame in a given data set using Time Series Analyzer V3 plugin, averaging the fluorescence in the ROI. The time courses were saved as txt files and fed into R scripts written by the authors to obtain the resting fluorescence data (averaged 30 frames before stimulus) and the  $\Delta F/F$  data (Supplementary File 2). Graphs were generated using GraphPad Prism 8. Figures were made using Adobe Illustrator.

### **Statistical analysis**

Data were analyzed in GraphPad Prism, using 2-way ANOVA, unpaired two-tailed Student's t-tests; graphs show mean  $\pm$  SEM, or Mann-Whitney U tests (for data not normally distributed); graphs show median with interquartile range. Pearson's correlation was used to examine relationships between datasets. Sample sizes are reported in figures.

## Results

### **The ER luminal Ca<sup>2+</sup> evoked response is more delayed and sustained compared to the cytoplasmic response**

To monitor Ca<sup>2+</sup> flux in the ER lumen, we generated transgenic flies that encoded ER-GCaMP6-210 (de Juan-Sanz et al. 2017), a GCaMP6 sensor fused to a signal peptide and ER retention signal, with a Ca<sup>2+</sup> affinity optimized for the relatively high [Ca<sup>2+</sup>] in ER lumen. ER-GCaMP6-210 localization in presynaptic terminals largely overlapped with the ER marker tdTomato::Sec61β (Fig. 1A), being more restricted than cytoplasmic jRCaMP1b (Fig. 1B; see comparison to ER marker Sturkopf::GFP, previously known as CG9186::GFP), consistent with localization to the ER lumen. To test the response of the sensor to neuronal activation we electrically stimulated the nerve. The cytoplasmic Ca<sup>2+</sup> response quickly reached a peak in the first couple of seconds following stimulation, and decayed back to resting levels over several seconds. In contrast, the ER-GCaMP6-210 luminal response increased more slowly, reaching a peak five or more seconds following stimulation, with a slow return to resting levels, in some cases over minutes (Fig. 2A,B; Supplementary Video 1), in keeping with the slower dynamics reported previously for these constructs (de Juan-Sanz et al. 2017). Cytoplasmically jRCaMP1b and GCaMP6f have similar kinetics in neurons as reported previously, with just a slightly slower half decay time (0.6s) for jRCaMP1b (Dana et al. 2016), compared to GCaMP6f (0.4s) (Chen et al. 2013) at 10 Hz. In around 10% of nerves, usually at higher stimulation frequencies, we alternatively (or sometimes additionally) observed small, sharp decreases in ER luminal fluorescence immediately following stimulation. This decrease was followed by a quick return to baseline fluorescence, or by a slow increase in fluorescence as described above. This short-term decrease in fluorescence was observed more frequently in the axon than at the NMJ. There did not appear to be anything notably different in the cytoplasmic flux in these instances, compared to when the ER flux showed only an increase in fluorescence (Fig. 2A; Fig. S1). Together this data suggests a slower and somewhat less predictable ER Ca<sup>2+</sup> flux, compared to the cytoplasmic flux in axons and NMJs of motor neurons.

### **ER luminal sensor with affinity closest to predicted ER luminal [Ca<sup>2+</sup>] shows the strongest response**

Since the high surface/volume ratio of the small ER tubules of axons might potentially make them more susceptible than other ER regions to leakage of Ca<sup>2+</sup> to the cytosol, we generated transgenic flies carrying two additional ER luminal sensors with higher Ca<sup>2+</sup> affinities. The highest affinity sensor, CEPIA3-ER (K<sub>d</sub>=11 μM), showed very small or no responses at multiple NMJs of seven larval preparations, even when a robust cytoplasmic response was elicited (not shown); CEPIA4-ER (K<sub>d</sub>=59 μM) usually showed a small response at most frequencies.

ER-GCaMP6-210 ( $K_d=210 \mu\text{M}$ ) produced the most consistent response, and the magnitude of its response increased with increasing stimulation frequency (Fig. 2B-D). As sensors with a  $K_d$  that approximates the surrounding  $[\text{Ca}^{2+}]$  are best suited as reporters, this is consistent with the estimated resting neuronal ER luminal  $[\text{Ca}^{2+}]$  of 150-200  $\mu\text{M}$  reported previously (de Juan-Sanz et al. 2017).

**The axonal cytoplasmic evoked response is smaller compared to NMJ response, whereas the ER luminal evoked response is consistent across locations**

As we were interested to see if we could observe  $\text{Ca}^{2+}$  signals along the length of the axon, we used *FMR-GMR27E09-GAL4* to record in the two Type Is motor neurons per hemisegment where it drives expression: RP2 and RP5, which together innervate several NMJs (Perez-Moreno and O'Kane 2019). We compared several axonal and NMJ locations within a muscle hemisegment (Fig. S2A). Motor neuron RP2 (also known as ISN-Is) innervates dorsal muscles, and we recorded from its NMJ boutons at muscle 1, and from two axonal locations: the "entry" point at which the axon starts to cross the muscles as it emerges from the ventral nerve cord, and more laterally as it passes over muscle 4. Motor neuron RP5 (also known as ISN b/d) innervates ventral muscles, and we recorded from its NMJ at muscle 6/7, and from one axonal location, the "entry" point, as defined for motor neuron RP2 (Fig. S2A,B; Supplementary Video 2). *Dpr-GMR94G06-GAL4* drives expression in the aCC Type Ib motor neuron (also known as MN1-Ib), which innervates muscle 1 (Perez-Moreno and O'Kane 2019). The responses of both cytosolic and luminal sensors at the aCC muscle 1 NMJ boutons were comparable to those in RP2 at the same muscle (Fig. 3A,B), suggesting a comparable action potential response between the two neuronal types. Fluorescence of the sensors driven by *Dpr-GMR94G06-GAL4* in the axons of the Type Ib aCC neuron was too dim to obtain reliable evoked responses, which may be due to a relatively small diameter of its axon, and hence relatively low amounts of sensors at this subcellular location.

The evoked cytoplasmic NMJ and axonal  $\text{Ca}^{2+}$  responses were both comparable between the two Type Is motor neurons, although axonal responses were consistently smaller than NMJ responses whereas ER luminal evoked responses were consistent across all NMJ and axonal locations (Fig. 3C). This did not appear to be due to alterations in ER volume as resting fluorescence was consistent across locations (Fig. S2C). Both cytoplasmic and ER luminal responses reached peak fluorescence on similar timescales across locations (Fig. 3D), suggesting that the observed responses were due to  $\text{Ca}^{2+}$  flux across the plasma membrane, and not a propagation of  $\text{Ca}^{2+}$  down the axon. The ER luminal response appeared in general not to be influenced by the cytoplasmic response; most locations showed no correlation of

peak  $\Delta F/F$  between ER lumen and cytosol, apart from RP2 axon at entry point (Fig. 3E,F, Table 2). This suggests a more complex transfer of  $Ca^{2+}$  within and between intracellular compartments, than simply a flow of  $Ca^{2+}$  from cytosol to ER lumen.

### ***Rtnl1*<sup>-</sup> *ReepA*<sup>-</sup> *ReepB*<sup>-</sup> mutants display an increased ER luminal evoked response compared to WT**

*Rtnl1*<sup>-</sup> *ReepA*<sup>-</sup> *ReepB*<sup>-</sup> mutant larvae have a disrupted axonal ER network, with larger and fewer tubules, and occasional fragmentation (Yalçın et al. 2017). To test whether these ER changes had functional consequences, we used *Dpr-GMR94G06-GAL4* to examine the cytoplasmic and ER lumen evoked responses at muscle 1 NMJ in these mutants. Mutant NMJs showed an increased evoked response compared to WT in the ER lumen, but not in the cytoplasm (Fig. 4A-B). There was no significant difference in lumen resting fluorescence between mutant and WT (Fig. 4C).

There was no correlation between cytoplasmic and ER luminal evoked responses in either mutant or WT at 40 Hz (Fig. S3), supporting the finding in Fig. 3 of a more complex intracellular transfer of calcium. It has been reported that ER lumen  $[Ca^{2+}]$  affects presynaptic cytoplasmic  $Ca^{2+}$  flux (de Juan-Sanz et al. 2017); however we found no correlation here between resting ER fluorescence and peak cytoplasmic fluorescence, in either WT or mutant stimulated at 40 Hz (Fig. S3). The time-to-peak in the cytoplasm or ER lumen was not significantly different between mutant and WT at 40 Hz (Fig. S4). The time for decay to half-maximal in the cytoplasm was also not significantly different between mutant and WT at 40 Hz (Fig. S4). This parameter was not measured in the ER lumen due to the slow temporal dynamics of this flux.

These data suggest a significant increase in ER luminal evoked responses in *Rtnl1*<sup>-</sup> *ReepA*<sup>-</sup> *ReepB*<sup>-</sup> mutants compared to WT, with no change in ER luminal resting fluorescence levels, no corresponding change in the cytoplasmic evoked response, and no change in the temporal dynamics of the response.

### **Discussion**

Direct measurement of ER luminal  $Ca^{2+}$  dynamics is essential for reporting on the physiological and pathophysiological responses of the ER network. An ER luminal *UAS-GEC1*, ER-GCaMP6-210, provided the most robust responses in *Drosophila* motor neurons (Fig. 2), in keeping with results in mammalian hippocampal neurons (de Juan-Sanz et al. 2017). Handler et al. (2019) also expressed this sensor in transgenic flies using a 10xUAS vector, and used these to detect  $Ca^{2+}$  release from the ER in mushroom body Kenyon cells. Our work provides a more detailed characterization of the responses of this sensor to a range

of stimulation frequencies, as well as providing an additional 17xUAS vector that we predict allows higher expression of the sensor.

In mutant *Drosophila* lacking various ER-shaping HSP protein homologs, we previously found decreased ER levels compared to WT, or occasional discontinuity of the ER network (Yalçın et al. 2017). As sustained discontinuity could potentially disrupt long-range ER communication along the axon, we wanted to investigate if we could record  $\text{Ca}^{2+}$  fluxes in WT axons. We analyzed both cytoplasmic and ER luminal  $\text{Ca}^{2+}$  fluxes, at three axonal recording positions across two neurons. The amplitude of the ER luminal evoked response was similar in axons and at the NMJ; however cytoplasmic evoked responses were smaller in axons compared to the NMJ. Even though  $\text{Ca}^{2+}$  would be fluxing across the ER membrane in response to stimulation, it appears that the two signals do not influence each other in most cases (Fig. 3).

While we observe  $\text{Ca}^{2+}$  signals along the length of motor axons, we do not find any indication of propagation via a  $\text{Ca}^{2+}$  wave. Propagation speeds for  $\text{Ca}^{2+}$  waves in dendrites have been measured at 60-90  $\mu\text{m/s}$  (Nakamura et al. 2002), with a rapid luminal  $\text{Ca}^{2+}$  diffusion through dendritic ER at  $\sim 30 \mu\text{m/s}$  (Choi et al. 2006). Here we find no evidence for any spatial differences in the time to peak fluorescence between different axon positions and the NMJ, both for ER lumen and cytoplasmic evoked responses (Fig. 3); in a typical video frame width of 100  $\mu\text{m}$  (e.g. Fig. S1, S2) we should easily detect propagation at these speeds with our frame rate of 10 Hz. The instantaneous spread of  $\text{Ca}^{2+}$  responses that we observe is more consistent with them being a consequence of the action potentials generated by stimulation, which propagate so fast that we cannot resolve their spread using our optical recording. Detection of  $\text{Ca}^{2+}$  waves that propagate along the ER membrane, or through the lumen would probably require recording of ER  $\text{Ca}^{2+}$  fluxes in the absence of action potentials.

Although the cytoplasmic evoked responses of *Rtnl1<sup>-</sup> ReepA<sup>-</sup> ReepB<sup>-</sup>* mutants were normal, the ER luminal evoked responses were significantly larger than WT (Fig. 4). This did not appear to be due to increased resting ER luminal  $[\text{Ca}^{2+}]$  since resting fluorescence levels showed no significant difference between genotypes, for either ER or cytoplasmic sensors.

In the simplest interpretation, the presynaptic ER lumen appears to take up more  $\text{Ca}^{2+}$  on stimulation in the *Rtnl1<sup>-</sup> ReepA<sup>-</sup> ReepB<sup>-</sup>* mutant compared to WT. Since cytoplasmic  $\text{Ca}^{2+}$  responses are unaffected in mutants, increased cytosolic  $\text{Ca}^{2+}$  cannot be an explanation for the increased ER response in mutants, implying that the increased ER response is due to intrinsic changes in  $\text{Ca}^{2+}$ -handling properties of the mutant ER, consistent with the roles of reticulon and REEP proteins in directly shaping ER architecture. The change in shape and composition of the ER tubules may change their flexibility (Georgiades et al. 2017) and effectiveness of ER tubule contraction (Holcman et al. 2018), hence a decrease in active flow,

thereby slowing the redistribution, and presenting as a transient increase in ER luminal  $\text{Ca}^{2+}$ . However as ER tubules have a larger diameter in mutant ER (Yalçın et al. 2017), this would work against this theory, as the larger tubules should enable active flow (Holcman et al. 2018). Alternatively, expression of ER  $\text{Ca}^{2+}$  proteins may be affected, such as the ER  $\text{Ca}^{2+}$  release channel RyR, highly expressed at axonal boutons (Sharp et al. 1993). If its expression levels were decreased, or its distribution altered, this could account for the lack of  $\text{Ca}^{2+}$  able to escape the lumen, and explain the transient increase in  $\text{Ca}^{2+}$  uptake observed on stimulation. Increased uptake of  $\text{Ca}^{2+}$  by mutant ER does not lead to decreased cytoplasmic  $[\text{Ca}^{2+}]$ ; however, we might not detect very local reductions in  $[\text{Ca}^{2+}]$  close to the ER, if masked by excess cytoplasmic fluorescence away from its immediate vicinity. Increasing bath  $[\text{Ca}^{2+}]$  can rescue transmitter release phenotypes in *atl* and *Rtnl1* mutants (Summerville et al. 2016); reducing bath  $[\text{Ca}^{2+}]$  in our setup might reveal cytoplasmic dysfunction not apparent at higher bath  $[\text{Ca}^{2+}]$ .

Could the increased ER luminal  $\text{Ca}^{2+}$  responses in mutants have any effects on cell physiology, if there is no corresponding increase in  $[\text{Ca}^{2+}]$  in the cytoplasm, where many  $\text{Ca}^{2+}$  effectors reside? There are  $\text{Ca}^{2+}$  effectors in the ER lumen such as calreticulin (Opas et al. 1991), although the protein-folding chaperone role of calreticulin is more likely to place its main function in rough rather than smooth ER. However, altered luminal  $\text{Ca}^{2+}$  responses could also affect physiology of organelles that obtain  $\text{Ca}^{2+}$  from the ER, including mitochondria and endo/lysosomal organelles (Raffaello et al. 2016). These effects could endure well beyond the original train of action potentials, due to the slow kinetics of  $\text{Ca}^{2+}$  uptake and release by the ER, with luminal  $[\text{Ca}^{2+}]$  not always returning to baseline during our recordings. Furthermore, aberrant ER  $\text{Ca}^{2+}$  handling has been postulated as a trigger for neurodegeneration, so what we are observing may well reflect deleterious changes in cellular health (Stutzmann and Mattson 2011, Ureshino et al. 2019). In support of our findings, mutation or knockdown of genes with a role in ER shaping, including *atl*, *Rtnl1* and *VAP*, also affect aspects of presynaptic function including neurotransmitter release and synaptic vesicle density, and the cytoplasmic presynaptic  $\text{Ca}^{2+}$  response (Summerville et al. 2016, De Gregorio et al. 2017, Lindhout et al. 2019). Given the number of HSP genes whose products localize to ER (Montenegro et al. 2012, Blackstone 2018) and could therefore affect  $\text{Ca}^{2+}$  dynamics, altered  $\text{Ca}^{2+}$  handling in axons or axonal terminals could potentially be a contributory factor to HSP pathology. Taken together, this data strongly suggests a role for ER in modulating presynaptic function, and highlights the importance of having an intact, functional ER network.

In conclusion, we have demonstrated the use of ER lumenally targeted GECIs for use in *Drosophila*, successfully recording fluxes at both the NMJ and in the axon. We have demonstrated the utility of these sensors in identifying functional differences between WT and

*Rtnl1*<sup>-</sup> *ReepA*<sup>-</sup> *ReepB*<sup>-</sup> mutant flies, whose axonal ER network it is known to be affected. We anticipate these will be useful additions to a *Drosophila* Ca<sup>2+</sup> imaging toolkit in the future, to further our understanding of HSP, and neurodegeneration more broadly.

In review

## **Conflict of Interest Statement**

The authors have no conflicts of interest to declare.

## **Author Contributions**

MKO performed all the cloning and Ca<sup>2+</sup> imaging experiments, and together with CJO'K designed the experiments. JJPM performed the confocal imaging acquisition. JO'S performed preliminary experiments and contributed to data analysis. TW provided initial training and support for Ca<sup>2+</sup> imaging experiments, and assisted in experimental design. The paper was written by MKO and CJO'K with comments and edits by JJPM, TJW and JO'S.

## **Funding**

This work was supported by grants BB/L021706 from the UK Biotechnology and Biological Sciences Research Council and MR/S011226 from the UK Medical Research Council to CJO'K. MKO was supported by a Newton International Fellowship (NF150362) from The Royal Society and a Marie Skłodowska-Curie Fellowship (701397) from the European Commission, JJPM was supported by a Marie Skłodowska-Curie fellowship (745007) from the European Commission.

## **Acknowledgments**

We thank The University of Cambridge Department of Genetics Fly Facility for providing the *Drosophila* microinjection service, Timothy Ryan for providing the FCK(1.3)GW-ER-GCaMP6-210 plasmid and Bloomington *Drosophila* Stock Centre for stocks.

This manuscript has been released as a pre-print at bioRxiv (Oliva et al. 2020).

## References

- Bischof, J., R. K. Maeda, M. Hediger, F. Karch and K. Basler (2007). An optimized transgenesis system for *Drosophila* using germ-line-specific phiC31 integrases. *Proc Natl Acad Sci U S A* 104, 3312-3317 DOI: 10.1073/pnas.0611511104.
- Blackstone, C. (2018). Converging cellular themes for the hereditary spastic paraplegias. *Curr Opin Neurobiol* 51, 139-146 DOI: 10.1016/j.conb.2018.04.025.
- Chen, T. W., T. J. Wardill, Y. Sun, S. R. Pulver, S. L. Renninger, A. Baohan, et al. (2013). Ultrasensitive fluorescent proteins for imaging neuronal activity. *Nature* 499, 295-300 DOI: 10.1038/nature12354.
- Choi, Y. M., S. H. Kim, S. Chung, D. Y. Uhm and M. K. Park (2006). Regional interaction of endoplasmic reticulum Ca<sup>2+</sup> signals between soma and dendrites through rapid luminal Ca<sup>2+</sup> diffusion. *J Neurosci* 26, 12127-12136 DOI: 10.1523/JNEUROSCI.3158-06.2006.
- Dana, H., B. Mohar, Y. Sun, S. Narayan, A. Gordus, J. P. Hasseman, et al. (2016). Sensitive red protein calcium indicators for imaging neural activity. *Elife* 5, e12727-e22751 DOI: 10.7554/eLife.12727.
- De Gregorio, C., R. Delgado, A. Ibacache, J. Sierralta and A. Couve (2017). *Drosophila* Atlantin in motor neurons is required for locomotion and presynaptic function. *J Cell Sci* 130, 3507-3516 DOI: 10.1242/jcs.201657.
- de Juan-Sanz, J., G. T. Holt, E. R. Schreiter, F. de Juan, D. S. Kim and T. A. Ryan (2017). Axonal Endoplasmic Reticulum Ca(2+) Content Controls Release Probability in CNS Nerve Terminals. *Neuron* 93, 867-881 DOI: 10.1016/j.neuron.2017.01.010.
- Edelstein, A. D., M. A. Tsuchida, N. Amodaj, H. Pinkard, R. D. Vale and N. Stuurman (2014). Advanced methods of microscope control using muManager software. *J Biol Methods* 1, e10-e20 DOI: 10.14440/jbm.2014.36.
- Fowler, P. C. and N. C. O'Sullivan (2016). ER-shaping proteins are required for ER and mitochondrial network organization in motor neurons. *Hum Mol Genet* 25, 2827-2837 DOI: 10.1093/hmg/ddw139.
- Georgiades, P., V. J. Allan, G. D. Wright, P. G. Woodman, P. Udommai, M. A. Chung, et al. (2017). The flexibility and dynamics of the tubules in the endoplasmic reticulum. *Sci Rep* 7, 16474-16484 DOI: 10.1038/s41598-017-16570-4.
- Handler, A., T. G. W. Graham, R. Cohn, I. Morantte, A. F. Siliciano, J. Zeng, et al. (2019). Distinct Dopamine Receptor Pathways Underlie the Temporal Sensitivity of Associative Learning. *Cell* 178, 60-75 e19 DOI: 10.1016/j.cell.2019.05.040.

Holcman, D., P. Parutto, J. E. Chambers, M. Fantham, L. J. Young, S. J. Marciniak, et al. (2018). Single particle trajectories reveal active endoplasmic reticulum luminal flow. *Nat Cell Biol* 20, 1118-1125 DOI: 10.1038/s41556-018-0192-2.

Li, J., B. Yan, H. Si, X. Peng, S. L. Zhang and J. Hu (2017). Atlastin regulates store-operated calcium entry for nerve growth factor-induced neurite outgrowth. *Sci Rep* 7-16, 43490 DOI: 10.1038/srep43490.

Lindhout, F. W., Y. Cao, J. T. Kevenaer, A. Bodzeta, R. Stucchi, M. M. Boumpoutsari, et al. (2019). VAP-SCRN1 interaction regulates dynamic endoplasmic reticulum remodeling and presynaptic function. *EMBO J* 38, e101345-e101362 DOI: 10.15252/embj.2018101345.

Macleod, G. T., M. Hegstrom-Wojtowicz, M. P. Charlton and H. L. Atwood (2002). Fast calcium signals in *Drosophila* motor neuron terminals. *J Neurophysiol* 88, 2659-2663 DOI: 10.1152/jn.00515.2002.

Montenegro, G., A. P. Rebelo, J. Connell, R. Allison, C. Babalini, M. D'Aloia, et al. (2012). Mutations in the ER-shaping protein reticulon 2 cause the axon-degenerative disorder hereditary spastic paraplegia type 12. *J Clin Invest* 122, 538-544 DOI: 10.1172/JCI60560.

Moreau, K., A. Fleming, S. Imarisio, A. Lopez Ramirez, J. L. Mercer, M. Jimenez-Sanchez, et al. (2014). PICALM modulates autophagy activity and tau accumulation. *Nat Commun* 5-24, 4998 DOI: 10.1038/ncomms5998.

Nakamura, T., N. Lasser-Ross, K. Nakamura and W. N. Ross (2002). Spatial segregation and interaction of calcium signalling mechanisms in rat hippocampal CA1 pyramidal neurons. *J Physiol* 543, 465-480 DOI: 10.1113/jphysiol.2002.020362.

O'Sullivan, N. C., T. R. Jahn, E. Reid and C. J. O'Kane (2012). Reticulon-like-1, the *Drosophila* orthologue of the hereditary spastic paraplegia gene reticulon 2, is required for organization of endoplasmic reticulum and of distal motor axons. *Hum Mol Genet* 21, 3356-3365 DOI: 10.1093/hmg/dds167.

Opas, M., E. Dziak, L. Fliegel and M. Michalak (1991). Regulation of expression and intracellular distribution of calreticulin, a major calcium binding protein of nonmuscle cells. *J Cell Physiol* 149, 160-171 DOI: 10.1002/jcp.1041490120.

Perez-Moreno, J. J. and C. J. O'Kane (2019). GAL4 Drivers Specific for Type Ib and Type Is Motor Neurons in *Drosophila*. *G3* 9, 453-462 DOI: 10.1534/g3.118.200809.

Pfeiffer, B. D., A. Jenett, A. S. Hammonds, T. T. Ngo, S. Misra, C. Murphy, et al. (2008). Tools for neuroanatomy and neurogenetics in *Drosophila*. *Proc Natl Acad Sci U S A* 105, 9715-9720 DOI: 10.1073/pnas.0803697105.

Raffaello, A., C. Mammucari, G. Gherardi and R. Rizzuto (2016). Calcium at the Center of Cell Signaling: Interplay between Endoplasmic Reticulum, Mitochondria, and Lysosomes. *Trends Biochem Sci* 41, 1035-1049 DOI: 10.1016/j.tibs.2016.09.001.

Schindelin, J., I. Arganda-Carreras, E. Frise, V. Kaynig, M. Longair, T. Pietzsch, et al. (2012). Fiji: an open-source platform for biological-image analysis. *Nat Methods* 9, 676-682 DOI: 10.1038/nmeth.2019.

Sharp, A. H., P. S. McPherson, T. M. Dawson, C. Aoki, K. P. Campbell and S. H. Snyder (1993). Differential immunohistochemical localization of inositol 1,4,5-trisphosphate- and ryanodine-sensitive Ca<sup>2+</sup> release channels in rat brain. *J Neurosci* 13, 3051-3063.

Stewart, B. A., H. L. Atwood, J. J. Renger, J. Wang and C. F. Wu (1994). Improved stability of *Drosophila* larval neuromuscular preparations in haemolymph-like physiological solutions. *J Comp Physiol A* 175, 179-191.

Stutzmann, G. E. and M. P. Mattson (2011). Endoplasmic reticulum Ca(2+) handling in excitable cells in health and disease. *Pharmacol Rev* 63, 700-727 DOI: 10.1124/pr.110.003814.

Summerville, J. B., J. F. Faust, E. Fan, D. Pendin, A. Daga, J. Formella, et al. (2016). The effects of ER morphology on synaptic structure and function in *Drosophila melanogaster*. *J Cell Sci* 129, 1635-1648 DOI: 10.1242/jcs.184929.

Suzuki, J., K. Kanemaru, K. Ishii, M. Ohkura, Y. Okubo and M. Iino (2014). Imaging intraorganellar Ca<sup>2+</sup> at subcellular resolution using CEPIA. *Nat Commun* 5, 4153-4166 DOI: 10.1038/ncomms5153.

Thiel, K., C. Heier, V. Haberl, P. J. Thul, M. Oberer, A. Lass, et al. (2013). The evolutionarily conserved protein CG9186 is associated with lipid droplets, required for their positioning and for fat storage. *J Cell Sci* 126, 2198-2212 DOI: 10.1242/jcs.120493.

Ureshino, R. P., A. G. Erustes, T. B. Bassani, P. Wachilewski, G. C. Guarache, A. C. Nascimento, et al. (2019). The Interplay between Ca(2+) Signaling Pathways and Neurodegeneration. *Int J Mol Sci* 20 DOI: 10.3390/ijms20236004.

Yalçın, B., L. Zhao, M. Stofanko, N. C. O'Sullivan, Z. H. Kang, A. Roost, et al. (2017). Modeling of axonal endoplasmic reticulum network by spastic paraplegia proteins. *Elife* 6, e23882-23899 DOI: 10.7554/eLife.23882.

## Figure Legends

**Fig 1.** The ER lumenal sensor ER-GCaMP6-210 has an overlapping distribution with ER at the neuromuscular junction. Panels show markers in Ib boutons at muscle 1 NMJ, segment A2, expressed using *Dpr-GMR94G06-GAL4*; all images are maximum intensity projections of confocal stacks. **(A)** Overlap of ER-GCaMP6-210 and ER membrane marker *tdTomato::Sec61β*. **(B)** jRCaMP1b is more broadly distributed than ER membrane marker *Sturkopf::GFP*. Magnified views of each inset are in respective lower rows.

**Fig 2.** ER lumenal  $\text{Ca}^{2+}$  responses to electrical stimulation at the NMJ, visualized using ER-GCaMP6-210, were delayed and more sustained compared to cytoplasmic responses. **(A)** Representative pseudocolour images of responses to 40 Hz stimulation, with maximal responses shown in grayscale (right panels) to show position of synapse. Panels show responses of jRCaMP1b (top row) and ER-GCaMP6-210 (bottom row) at muscle 6/7, expressed in the same RP5 Type Is motor neuron using *FMR-GMR27E09-GAL4*. Arrows show examples of boutons. Pseudocolour bar shows low to high relative intensity; scale bar, 2  $\mu\text{m}$ . **(B)** Representative responses to 20 Hz stimulation, of ER-GCaMP6-210 and CEPIA4-ER with corresponding jRCaMP1b response at muscle 6/7, expressed in RP5 Type Is motor neuron using *FMR-GMR27E09-GAL4*. Shading represents the stimulation period. **(C)** Average fold-change in peak fluorescence at different stimulation frequencies, of ER-GCaMP6-210 (green) and CEPIA4-ER, compared with jRCaMP1b (magenta) at muscle 6/7, expressed in the same RP5 Type Is motor neuron using *FMR-GMR27E09-GAL4*. (ER-GCaMP6-210, N=5; CEPIA4-ER, N=6). **(D)** Comparison of ER lumenal sensors only, replotted from **(C)** with the y-axis expanded.

**Fig 3.** Comparisons of ER lumenal and cytoplasmic  $\text{Ca}^{2+}$  responses across axons and NMJs of Type Ib and Is motor neurons. **(A)** Evoked responses of lumenal ER-GCaMP6-210 and cytoplasmic jRCaMP1b to a range of stimulation frequencies, in Type Ib boutons of the aCC neuron at the muscle 1 NMJ, expressed using *Dpr-GMR94G06-GAL4* (N=6), or in Type Is boutons at the muscle 1 NMJ of the RP2 neuron expressed using *FMR-GMR27E09-GAL4* (N=6). **(B)** Comparison of ER lumen sensor data only, from **(A)** but with y-axis expanded. **(C)** Lumen and cytoplasmic  $\text{Ca}^{2+}$  fluxes at different positions of Type Is neurons RP2 and RP5 (Fig. S2A), with sensors expressed using *FMR-GMR27E09-GAL4*. **(D)** The time to peak  $\Delta F/F$ , for both lumen and cytoplasmic responses, was similar across all axon and NMJ positions. **(E, F)** Peak amplitudes (from **(C)**) of individual ER lumen and cytoplasm responses were plotted for the NMJ **(E)** and axonal **(F)** compartments of RP2 and RP5. A positive correlation was

found only for RP2 axon entry but not for other locations (Table 2). One outlier in RP2 axon (muscle 4) jRCaMP1b was excluded from graphs (C) and (F) (value 0.29), but included in analysis in (F).

**Fig 4.** ER luminal, but not cytoplasmic responses, were significantly increased in *RtnI1<sup>-</sup> ReepA<sup>-</sup> ReepB<sup>-</sup>* mutant Type Ib boutons compared to *WT*, with no difference in resting fluorescence intensity. (A) Luminal ER-GCaMP6-210 expressed in aCC using *Dpr-GMR94G06-GAL4*, showed a larger evoked response in Type Ib NMJs at muscle 1 in mutants, compared to *WT*. 40 Hz stimulation panel shows the maximum response of the given GECI following stimulation. GECIs were co-expressed in the same neuron. Pseudocolour bar (for  $\Delta F/F$  panels) shows low to high  $\Delta F/F$ ; scale bar, 5  $\mu\text{m}$ . (B) There was no significant difference between mutant (N=13 larvae) and *WT* (N=14 larvae) in cytoplasmic responses (jRCaMP1b) at these boutons stimulated over a range of frequencies, but there was a significant increase in the ER luminal response (2-way ANOVA). The lower graph shows the ER luminal response only, with the y-axis expanded. (C) There was no significant effect of the triple mutant on the resting fluorescence intensity (from the 40 Hz recording) of either sensor (Mann-Whitney U test).

Table 1: Stocks and plasmids used in this work

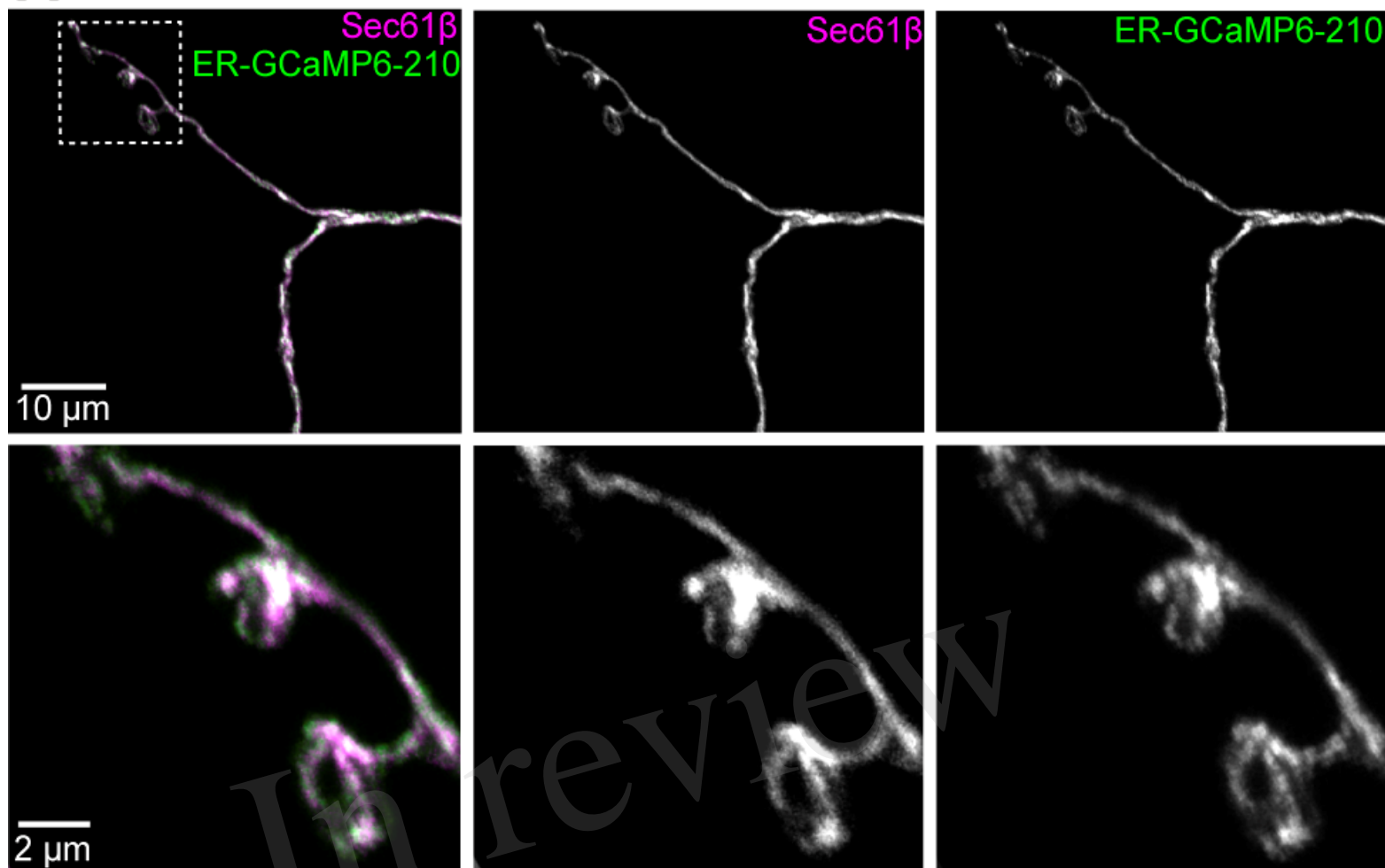
<b>Drosophila Stock Genotype</b>	<b>RRID</b>	<b>Source/Reference</b>
<i>y w; +; 17xUASTattB-ER-GCaMP6-210(attP86Fb)</i>	-	This paper
<i>y w; +; 17xUASTattB-CEPIA3-ER(attP86Fb)</i>	-	This paper
<i>y w; +; 17xUASTattB-CEPIA4-ER(attP86Fb)</i>	-	This paper
<i>w<sup>1118</sup>; +; UAS-tdTomato::Sec61β(attP2)</i>	BDSC_64747	(Summerville et al. 2016)
<i>w; UAS-Sturkopf::GFP; +</i> (Formerly <i>UAS-CG9186::GFP</i> )	-	(Thiel et al. 2013) (Yalçın et al. 2017)
<i>w; +; UAS-jRCaMP1b(VK00005)</i>	BDSC_63793	(Dana et al. 2016)
<i>w; Rtnl1<sup>-</sup> ReepA<sup>-</sup> ReepB/CyO; +</i>	BDSC_77904	(Yalçın et al. 2017)
<i>w; ReepA+; + (WT control)</i>	-	(Yalçın et al. 2017)
<i>w<sup>1118</sup>; +; Dpr-GMR94G06-GAL4(attP2)</i>	BDSC_40701	(Pfeiffer et al. 2008, Perez-Moreno and O'Kane 2019)
<i>w<sup>1118</sup>; +; FMR-GMR27E09-GAL4(attP2)</i>	BDSC_49227	(Pfeiffer et al. 2008, Perez-Moreno and O'Kane 2019)
<b>Plasmid</b>		
<i>ER-GCaMP6-210</i>	Addgene_86919	Tim Ryan (de Juan-Sanz et al. 2017)
<i>pCMV CEPIA3mt</i>	Addgene_58219	Masamitsu lino (Suzuki et al. 2014)
<i>pCMV CEPIA4mt</i>	Addgene_58220	Masamitsu lino (Suzuki et al. 2014)
<i>p17xUASTattB</i>	-	This paper
<i>p17xUASTattB-ER-GCaMP6-210</i>	-	This paper
<i>p17xUASTattB-CEPIA3-ER</i>	-	This paper
<i>p17xUASTattB-CEPIA4-ER</i>	-	This paper

Table 2: Correlation analysis of peak  $\Delta F/F$  between ER lumen and cytosol in NMJ and axons using Pearson's correlation coefficient.

<b>FMR-GMR27E09 Neuronal location</b>	<b>r</b>	<b>p</b>	<b>N (larvae)</b>
RP2 NMJ muscle 1	0.10	0.85	6
RP5 NMJ muscle 6/7	0.21	0.73	5
RP2 axon (entry)	0.98	0.02*	4
RP2 axon (muscle 4)	0.50	0.32	6
RP5 axon (entry)	0.23	0.77	4

# Figure 1 - single column

**A**



**B**

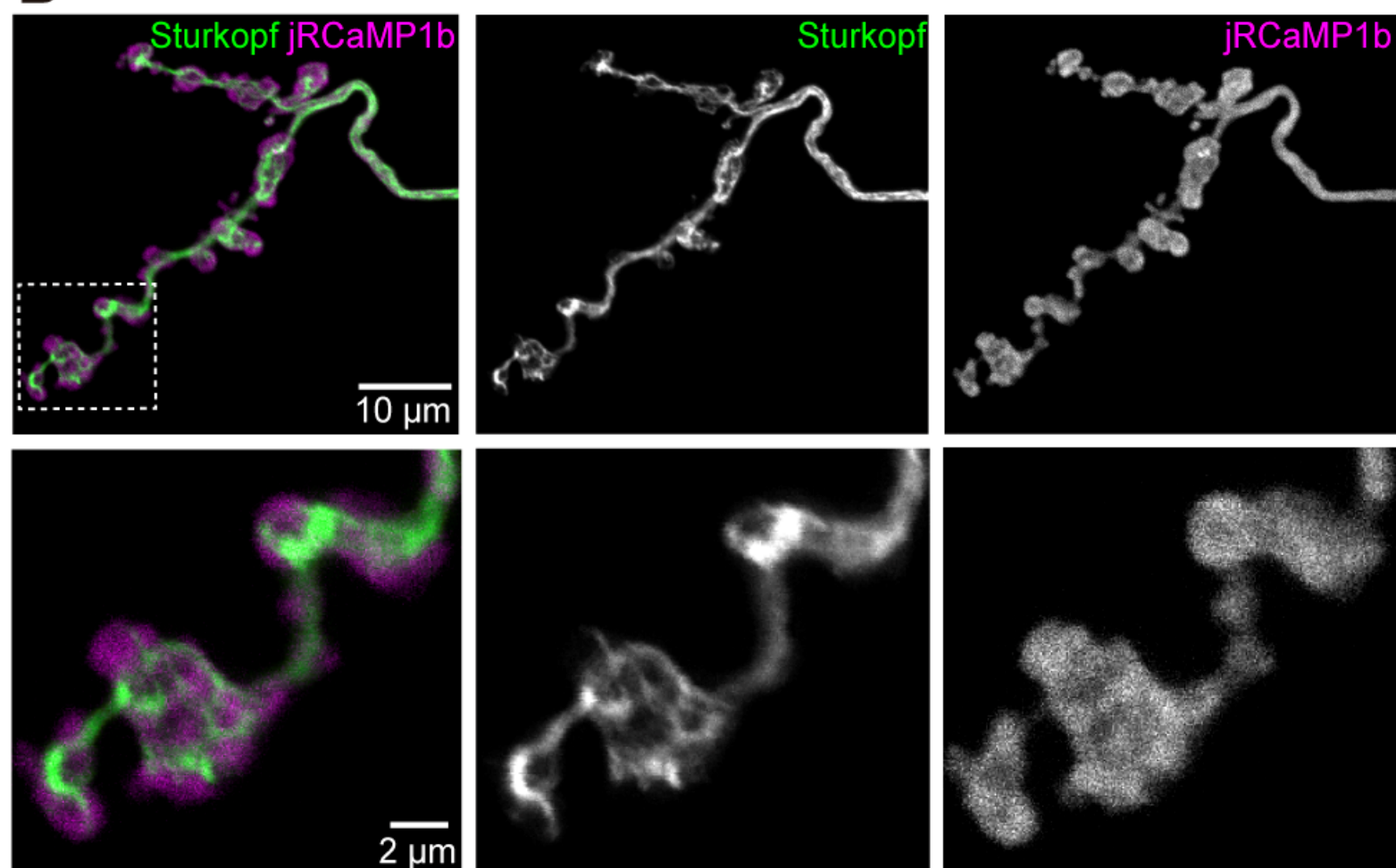


## Figure 2 - 2 column

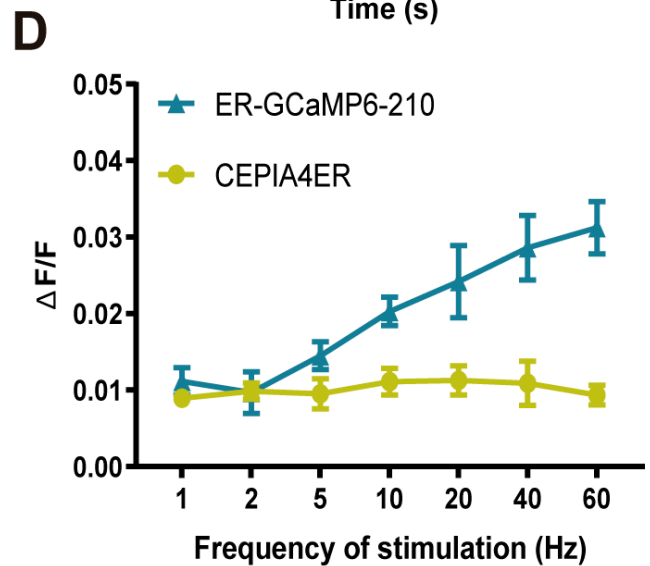
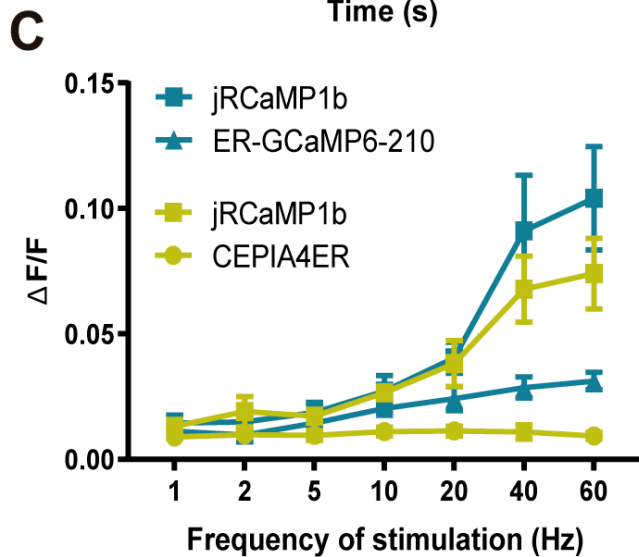
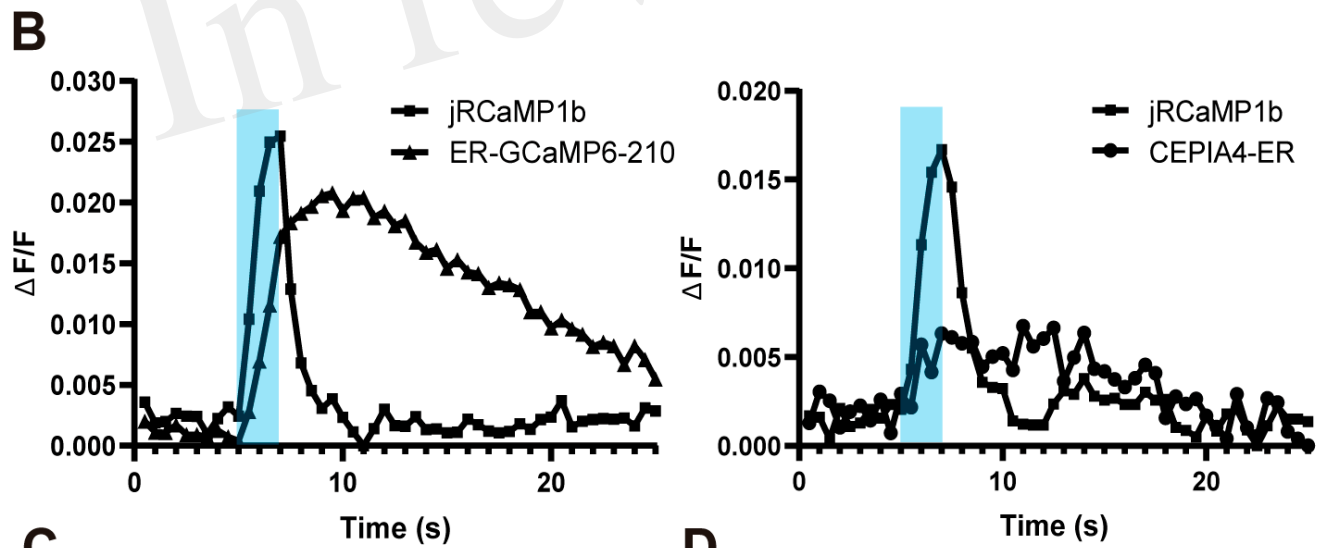
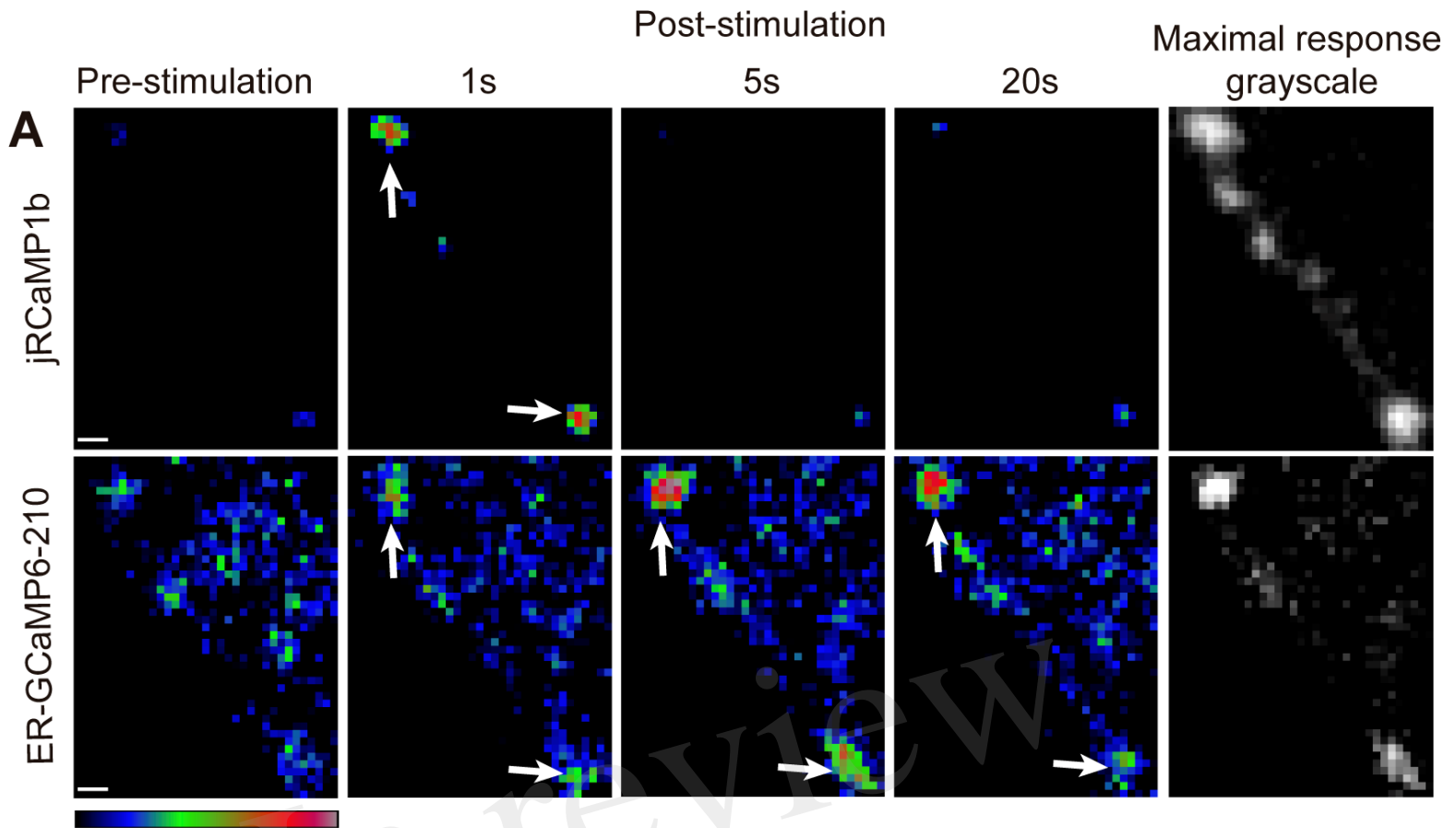


**Figure 3 - double column**

Figure 3.111

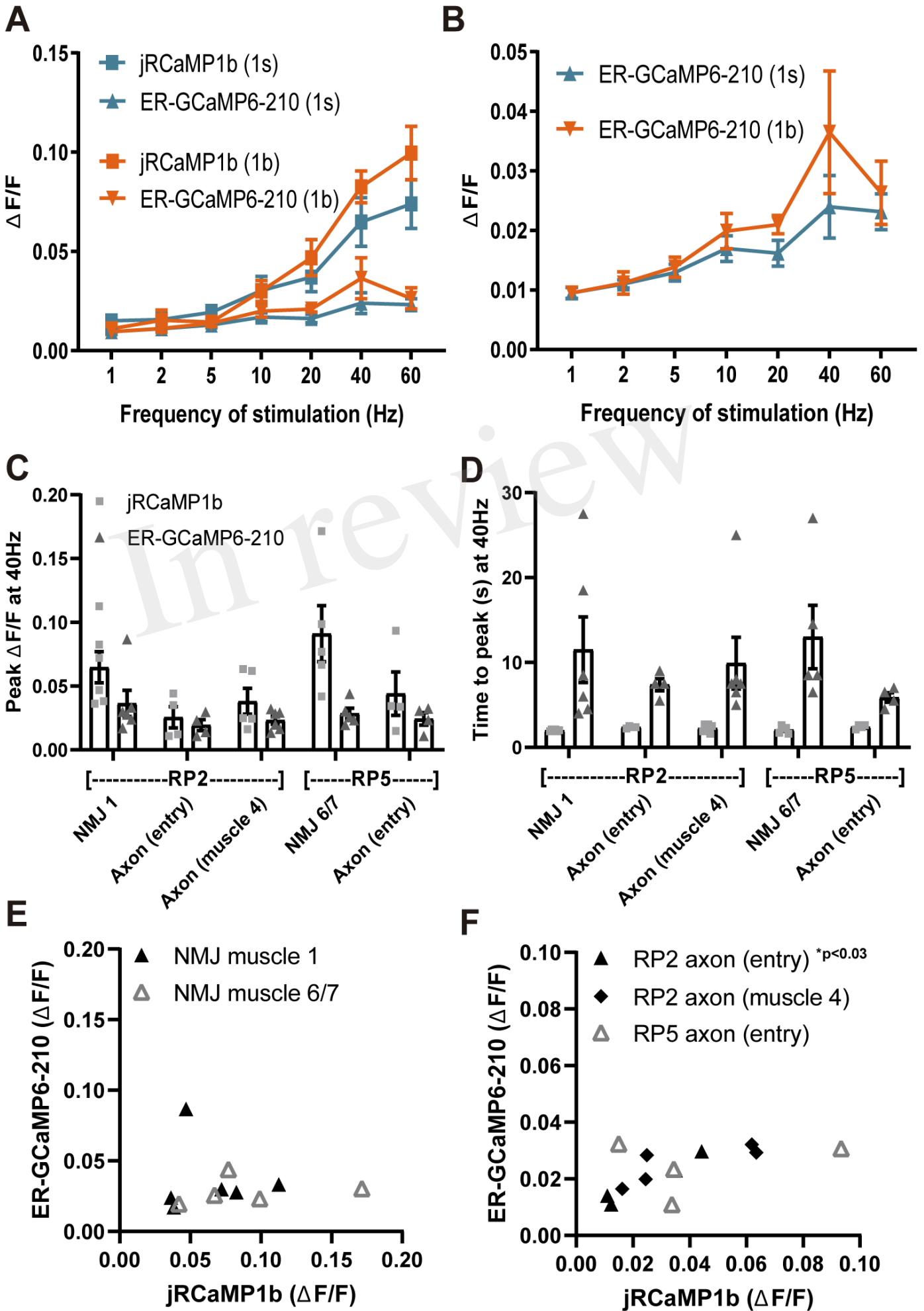


**Figure 4 - 1 column**

Figure 4.TIF

